Integrin-associated Protein Immunoglobulin Domain Is Necessary for Efficient Vitronectin Bead Binding

Frederik P. Lindberg,*‡ Hattie D. Gresham,‖ Martina I. Reinhold,* and Eric J. Brown*‡§

Departments of *Infectious Diseases, ‡Molecular Microbiology, and §Cell Biology and Physiology, Washington University School of Medicine, St. Louis, Missouri 63110; and ‖Research Service, Harry S. Truman Veterans Affairs Medical Center, Columbia, Missouri 65201

Abstract. Integrin-associated protein (IAP/CD47) is physically associated with the $\alpha_v\beta_3$ vitronectin (Vn) receptor and a functionally and immunologically related integrin on neutrophils (PMN) and monocytes. Anti-IAP antibodies inhibit multiple phagocyte functions, including Arg-Gly-Asp (RGD)–initiated activation of phagocytosis, chemotaxis, and respiratory burst; PMN adhesion to entactin; and PMN transendothelial and transepithelial migration at a step subsequent to tight intercellular adhesion. Anti-IAP antibodies also inhibit binding of Vn-coated particles to many cells expressing $\alpha_v\beta_3$. However, prior studies with anti-IAP did not directly address IAP function because they could not distinguish between IAP blockade and antibody-induced signaling effects on cells. To better determine the function of IAP, we have characterized and used an IAP-deficient human cell line. Despite expressing α_v integrins, these cells do not bind Vn-coated particles unless transfected with IAP expression constructs. Increasing the level of $\alpha_v\beta_3$ expression or increasing Vn density on the particle does not overcome the requirement for IAP. All known splice variants of IAP restore Vn particle binding equivalently. Indeed, the membrane-anchored IAP Ig variable domain suffices to mediate Vn particle binding in this system, while the multiply membrane-spanning and cytoplasmic domains are dispensable. In all cases, adhesion to a Vn-coated surface and fibronectin particle binding through $\alpha_5\beta_1$ fibronectin receptors are independent of IAP expression. These data demonstrate that some α_v integrin ligand-binding functions are IAP independent, whereas others require IAP, presumably through direct physical interaction between its Ig domain and the integrin.

INTEGRINS are heterodimeric cell surface receptors that mediate binding to other cells and to ligands in the extracellular matrix. Integrin-dependent ligand binding and clustering-induced signal transduction lead to changes in cell morphology and activation state. Conversely, signals inside the cell can result in changes in integrin ligand affinity and avidity. One of the proteins implicated in these regulatory events is integrin-associated protein (IAP).[1]

IAP is a unique Ig family member with an amino-terminal Ig variable (IgV) domain, a multiply membrane-spanning domain, and a short alternatively spliced carboxy-terminal cytoplasmic tail (Lindberg et al., 1993; Reinhold et al., 1995). IAP is identical to OA-3, an ovarian carcinoma antigen, and to CD47, an erythrocyte membrane protein decreased in Rh_{null} disease (Campbell et al., 1992; Lindberg et al., 1994; Mawby et al., 1994). Since IAP is ubiquitously expressed (Brown et al., 1990; Rosales et al., 1992; Reinhold et al., 1995), its function has been inferred from the effect of antibody inhibition, mainly in myeloid and endothelial cells.

IAP was first identified as the target of antibodies that block extracellular matrix–induced activation of neutrophils (PMN) and monocytes (Brown et al., 1990). Anti-IAP mAbs also inhibit PMN transendothelial migration, PMN and endothelial cell chemotaxis to RGD-containing proteins, and PMN adhesion to entactin (Cooper et al., 1995; Senior et al., 1992). In addition, anti-IAP mAbs inhibit an increase in intracellular calcium concentration seen when endothelial cells spread on vitronectin (Vn) in an α_v-dependent manner (Schwartz et al., 1993). These studies all suggest that IAP interacts functionally with the integrin $\alpha_v\beta_3$, a hypothesis supported by physical association of the two molecules (Brown et al., 1990). Moreover,

Address all correspondence to Frederik P. Lindberg, Infectious Diseases Division, Campus Box 8051, Washington University School of Medicine, 660 S. Euclid Avenue, St. Louis, MO 63110. Tel.: (314) 362-2125. Fax: (314) 362-9185. e-mail:lindberg@id.wustl.edu.

1. *Abbreviations used in this paper*: DAF, decay-accelerating factor; Fn, fibronectin; GPI, glycosylphatidylinositol; HSA, human serum albumin; IAP, integrin-associated protein; IgV, Ig variable; IMDM, Iscove's modified Dulbecco's medium; PI-PLC, phosphoinositide phosopholipase C; PMN, neutrophil; TS-1, thrombospondin-1; Vn, vitronectin.

anti-IAP mAb inhibits the binding of Vn-coated particles to $\alpha_v\beta_3$ integrin on a variety of cells in addition to myeloid and endothelial cells (Lindberg et al., 1993).

Studies on the mechanisms by which IAP cooperates with $\alpha_v\beta_3$ or by which anti-IAP mAb inhibit various $\alpha_v\beta_3$ functions have been hampered by the ubiquity of IAP on tissue-culture cells. We have used an IAP-deficient ovarian carcinoma cell line, OV10, to better understand IAP–$\alpha_v\beta_3$ cooperation. Although adhesion of these cells to a Vn-coated surface is normal, they bind Vn-opsonized beads only if they are made to express IAP by transfection. We show that Vn-bead binding is IAP and integrin dependent and correlates with the level of both integrin and IAP expression. We also demonstrate that the IAP IgV domain is sufficient for this function. As OV10 adhesion to Vn on a surface is unaffected by expression of IAP, our data demonstrate a clear distinction between two different functions of α_v integrins: binding of Vn-beads, which is IAP dependent, and adhesion to a Vn-coated surface, which is IAP independent.

Materials and Methods

Chemicals, Reagents, and Antibodies

All reagents were of the highest grade commercially available and purchased from Sigma Chemical Co. (St. Louis, MO), unless otherwise indicated. PBS and HBSS were purchased as 10× stocks from Life Technologies/GIBCO BRL (Gaithersburg, MD) or BioWhittaker, Inc. (Walkersville, MD). Negative control mAb 6F2, anti-β_3 mAb 7G2, and anti-IAP mAbs B6H12 and 2D3 are all mouse IgG*1* mAbs and have been described previously (Gresham et al., 1989; Brown et al., 1990). None of these mAbs bind the corresponding murine antigens. Anti-α_v mAb L230 (Weinacker et al., 1994) was kindly provided by Dr. Dean Sheppard (University of California at San Francisco), and anti-LIBS1 (Frelinger et al., 1990) was kindly provided by Dr. Mark Ginsberg (The Scripps Research Institute, La Jolla, CA). Control IgG*1* mAb MOPC21 was from Organon-Teknika (Durham, NC). Anti-β_1 mAb P4C10 (IgG*1*) and anti-$\alpha_v\beta_5$ mAb P1F6 (IgG*1*) (Wayner et al., 1991), as well as rabbit polyclonal anti-human vitronectin receptor, were from Life Technologies/GIBCO BRL. Vn was purchased from Life Technologies/GIBCO BRL and Calbiochem-Novabiochem Corp. (La Jolla, CA). Fluorescinated anti-CD4-IgV_1 mAb OKT4A was purchased from Ortho Diagnostics (Raritan, NJ).

Tissue Culture

OVM1 and OV10 were maintained in Iscove's modified Dulbecco's medium (IMDM) (Life Technologies/GIBCO BRL) with 10% FCS (Hyclone Laboratories, Logan, UT) and 50 μg/ml gentamicin. Transfectants based on pRC/RSV or pIAP58 (Invitrogen, San Diego, CA) (Lindberg et al., 1993) were isolated and maintained in 400 μg/ml geneticin/G418 (Life Technologies/GIBCO BRL). Those based on pREP10 (Invitrogen) were selected in 200 μg/ml hygromycin (Boehringer Mannheim Biochemicals, Indianapolis, IN); those based on pSRαEN (a kind gift of Andrey Shaw, Washington University, St. Louis, MO) were selected in 800 μg/ml geneticin. Double transfectants were maintained in medium with 100 μg/ml hygromycin and 400 μg/ml geneticin. For vitronectin bead binding assays, cells were seeded at 20,000 cells per well into glass 8-chambered slides (LabTek; Nunc, Naperville, IL) in 250 μl RPMI (BioWhittaker, Inc.) with 10% FCS, 10 mM Hepes, and selective antibiotics at the concentrations stated above.

Flow Cytometry and Cell Sorting

Cells were removed from subconfluent tissue-culture flasks with PBS–2 mM EDTA, washed twice in complete medium, and counted. 1–3 million cells were resuspended in 25 μl complete medium with 1–3 μg antibody (saturating amounts) and incubated on ice for 30 min. Cells were washed and incubated with 50 μl complete medium with 1 μl goat anti–mouse IgG-FITC (F-7506; Sigma Chemical Co.), and then incubated an additional 30 min. After a wash, cells were analyzed on a flow cytometer (Epics/XL; Coulter Electronics, Inc., Hialeah, FL). For cell sorting, 15 million cells were stained with proportionately larger amounts of medium and antibody, resuspended at 5 million cells per ml, and sorted on a fluorescence-activated cell sorter (Epics 743; Coulter Electronics, Inc.).

Selection of an IAP-deficient Cell Line

The ovarian carcinoma line OVM1, kindly provided by Dr. Stimson (Strathclyde University, Glasgow, UK), was described as CD47 deficient by Campbell et al. (1992). The cells we obtained contained a small proportion (0.5–1%) of IAP-positive cells. Therefore, we cloned this cell line and selected numerous IAP-deficient clones from it. After tests of transfectability, the clone OV10 was chosen for further study. OV10 is IAP deficient by FACS® and immunoprecipitation with all our IAP mAbs, negative by immunoprecipitation with polyclonal rabbit anti-IAP carboxy-terminal peptide antisera (Lindberg et al., 1993), and negative for IAP mRNA by Northern blot and reverse-transcriptase PCR assays (not shown). We have been unable to detect spontaneous IAP-positive cells in OV10 populations. OV10 express a small amount of $\alpha_v\beta_3$, a moderate amount of $\alpha_v\beta_5$ (Table I), and a large amount of $\alpha_5\beta_1$ (not shown).

IAP Expression Constructs and Transfectants

IAP alternative splice variants are referred to as IAP-1 through IAP-4 in order of increasing cytoplasmic tail length (Reinhold et al., 1995). The pRC/RSV-based vector pIAP58 and the pIAP58-derived expression constructs pIAP45 (IAP-2), pIAP71 (IAP-1), and pIAP83 (mIAP; murine IAP-2) have been described previously (Lindberg et al., 1993). The IAP-4 expression construct pIAP120 was constructed in analogy with pIAP71, except that the 3′-portion of the cDNA was derived from an IAP-4 clone. The 3′-fragment of the IAP-3 expression construct pIAP131 was constructed from the IAP-4 version by PCR-mediated deletion of the 3′-end of the coding sequence, to correspond to the published IAP-3 sequence (Lindberg et al., 1993; Campbell et al., 1992; Reinhold et al., 1995). The IAP coding sequence of all constructs has been verified by dideoxynucleotide chain-termination sequencing (Sanger et al., 1977). The constructs were transfected into OV10 using the lipofectin method (Life Technologies/GIBCO BRL). Clones were isolated by limiting dilution 24 h after transfection. Several clones of the vector and IAP-2 transfectants were assayed with similar results. In some cases, clones were FACS® sorted to remove populations of lower expression. The clones presented in this study are 58A2 (vector), 71E3 (IAP-1), 45B10 (IAP-2), 131G7 (IAP-3), 120B9 (IAP-4), and 83E7 (mIAP).

The IAP–glycosylphosphatidylinositol (GPI) construct pIAP148 was constructed by cloning the IAP 5′-end up to and including the IgV domain as a XbaI–PvuII fragment and a PvuII–HindIII fragment encoding the human decay-accelerating factor (DAF) GPI signal (Medof et al., 1987) (kindly provided by Dr. Douglas Lublin, Washington University, St. Louis, MO) into XbaI–HindIII-digested pIAP58 vector. The fragment encoding the GPI signal was generated by PCR using the following oligonucleotides: AACCCTGCAGCTGGCATGAAACAACCCCA and CAATGAAAGCTTCCTAAATGAAGAG. Conversely, the sequence coding for the IAP-2 membrane and cytoplasmic domains was isolated from pIAP70 (Lindberg et al., 1993) and fused with a PCR-generated HindIII–PvuII fragment of the 5′-end of human CD4 (kindly provided by Dr. Andrey Shaw) up to and including the first IgV domain, yielding the plasmid pIAP147. The oligonucleotides used were: TGGTCTAGATGTCCCTACTGCTCAGCC and GTCAATCCGCTGCAGCTGAATTGCACCTCCTC. Transfectant clones were generated as described above. The clones used in this study were 148A10T (IAP-GPI) and 147E9 (CD4-IAP). To verify results obtained with IAP-GPI, two additional independent transfectants (148C11 and 148D12) were analyzed.

For higher IAP expression, the insert from pIAP45 (IAP-2) was cloned as an XhoI–XbaI fragment into the monocistronic vector pBSRαEN (kindly provided by Dr. Andrey Shaw), yielding pIAP315. Also, a construct encoding the IAP-IgV domain linked to a single membrane-spanning segment was made in the following manner: oligonucleotides CCTGGGGCGGATCCACCAAGGGCCTCTGCC and ACTGTCTGCCATCTAGAGCGTCCTCGCCAG were used in PCR on a CD16-CD7-syk construct (Kolanus et al., 1993) (kindly provided by Dr. Brian Seed, Massachusetts General Hospital, Boston, MA), yielding the CD7 membrane-spanning segment as a BamHI–XbaI fragment. This was fused with an XhoI–BamHI fragment of IAP cDNA (obtained by PCR with oligonucleotides CGCTCGAGAAACGATGTGGCCCCTGGTAG and TCATTTGGAT-

CCACCAGCTGACTAA from pIAP3 [Lindberg et al., 1993]) and cloned into pBSRαEN, yielding pIAP323. In both cases, a single round of FACS® sorting yielded a population with high expression in a narrow distribution. These populations were designated IAP-2(hi) (pIAP315) and IAP-TM (pIAP323).

To obtain OV10 transfectants with increased expression of integrin $\alpha_v\beta_3$, a β_3 expression plasmid was constructed by ligating the human integrin β_3 cDNA as an XbaI fragment into NheI-digested pREP10 (Invitrogen), yielding pIAP164. Transfecting this construct into OV10 with or without a 20-fold excess of pCDM8-α_v (Loftus et al., 1990), and selecting for hygromycin resistance, resulted in equivalent average levels of $\alpha_v\beta_3$ expression with a corresponding increase in surface expression of α_v (as assayed by FACS® with mAbs AP3 and L230; Table I). This suggests that β chain synthesis limits $\alpha_v\beta_3$ expression. One clone of pIAP164-transfected OV10 (OV10/164-10) was chosen and transfected in a second step with previously described IAP constructs, followed by geneticin selection and cloning. The transfectant clones used are: β_3/vector (pIAP164+ pIAP58B3), β_3/IAP-2 (pIAP164+45S2), and β_3/IAP-GPI (pIAP164+ pIAP148C2), to yield cells expressing high amounts of $\alpha_v\beta_3$ without IAP, with wild-type IAP, or with the IAP IgV domain on a GPI anchor, respectively.

Bead Binding

Confluent monolayers of OV10 transfectants were removed with trypsin-EDTA, washed in complete medium, and resuspended at 20,000 cells per ml in RPMI-based selection media (RPMI with 10% FCS, 400 μg/ml G418, and/or 100 μg/ml hygromycin, depending on the transfectant). Cell suspensions were added to glass 8-chamber LabTek slides and cultured for 24 h at 37°C in 5% CO_2. Vn-bead binding was optimal in a buffer of HBSS containing 10 mM Hepes, 0. 1 mM $MnCl_2$, and 1% human serum albumin (HSA) (bead-binding buffer), which was used for all studies. Adherent cells were washed twice with buffer and incubated with antibodies in 250 μl buffer for 20 min at room temperature. The antibodies used were MOPC21, anti-IAP mAb 2D3 and B6H12 (Brown et al., 1990), anti-β_3 mAb 7G2 (Gresham et al., 1989; Brown et al., 1990), and anti-$\alpha_v\beta_5$ mAb P1F6 (Wayner et al., 1991) all at 10 μg per well, as well as anti-β_1 P4C10 (1:50 dilution of ascites). After incubation with the antibodies, the adherent cells were washed twice, and 250 μl buffer was added to each well. Vn- and HSA-coated beads were made exactly as described (Lindberg et al., 1993), except that the source of the Vn was Life Technologies/GIBCO BRL or Calbiochem-Novabiochem Corp. The cells were incubated with either 20 μl Vn- or HSA-coated beads. For β_3 transfectants in Fig. 5, *A* and *C*, the volume of beads was reduced to 5 μl to facilitate counting of attached beads. After 1 h at 37°C, unbound beads were washed away, and the number of beads bound was assessed by fluorescence microscopy. Binding was quantitated as an attachment index, the number of beads bound per 100 cells.

Assay for Ligand-induced Binding Sites

OV10 transfectants were harvested in PBS–2 mM EDTA, washed twice in HBSS without divalent cations, and resuspended to 2 million cells per ml in bead-binding buffer or in bead-binding buffer with 5 mM $MgCl_2$ rather than 0. 1 mM $MnCl_2$. Human IgG (500 μg/ml) was used to further reduce nonspecific binding. 100-μl aliquots were incubated 30 min at room temperature with anti-LIBS1 (10 μ/ml) (Frelinger et al., 1990) and KYAVT-**GRGDS** at varying concentrations. After two washes, cells were stained with FITC-labeled secondary antibody and analyzed by flow cytometry.

Adhesion Assays

Flat-bottom 96-well microtiter plates (Immulon2; Dynatech Laboratories, Inc., Chantilly, VA) were coated overnight (4°C) with matrix protein in PBS, blocked for 1 h or more with PBS/1% HSA at room temperature, and washed twice with HBSS without divalent cations (HBSS--) before cell addition. Subconfluent monolayers were removed with PBS/5 mM EDTA twice in IMDM (without FCS) and incubated at 3 million cells per ml for 15 min (37°C) in IMDM–1% BSA containing 3 μM calcein-AM (Molecular Probes, Eugene, OR). Cells were washed twice in HBSS--, followed by resuspension in bead-binding buffer (HBSS/0. 1 mM $MnCl_2$/1% HSA) at 1 million cells per ml. Cells were diluted 1:2 in buffer containing the appropriate blocking mAb, preincubated for 10 min at room temperature, and added to the microtiter plates at 100 μl per well (50,000 cells). After 60 min at 37°C, fluorescence was read on a plate reader (excitation 485 nm, emission 530 nm; Cytofluor 2300; Millipore Corp., Bedford, MA) before and after two washes with adhesion buffer. Data are given as the fraction of total fluorescence that was retained through the washes.

Maximal adhesion obtained with any substrate was ~80%, with background from blocked wells <2%.

Phosphoinositide Phospholipase C Treatment

Confluent monolayers of cells were removed with trypsin-EDTA, washed in complete IMDM with 10 mM EDTA, and resuspended in the same medium to 3 million cells per ml. 0.5-ml aliquots were incubated with or without the addition of 0.1 U of phosphoinositide phospholipase C (PI-PLC) (Boehringer Mannheim Biochemicals) for 1 h at 37°C. Volumes of 0.1 ml were pelleted in microtiter plates, washed, and processed for flow cytometry after staining with negative control mAb 6F2 or anti-IAP mAbs 2D3 or 1F7. Both anti-IAP mAbs gave identical results.

IAP-β_3 Coimmunoprecipitation

Cells were grown to subconfluence, harvested by scraping, and washed three times in HBSS--. 40 million cells (routinely >98% intact by trypan blue exclusion) were lysed in 1 ml 0.25 M sucrose/50 mM Hepes (pH 7.4)/ 100 mM octylglucoside with protease inhibitors (5 mM iodoacetamide, 1 mM PMSF, 50 μg/ml aprotinin, 50 μg/ml leupeptin) by rotation for 2 h at 4°C. Lysates were cleared by a 30-min centrifugation (15,000 *g*) at 4°C. Equal fractions of the lysate were rotated at 4°C with 50 μl anti-IAP (2D3), anti-β_3 (7G2), or anti-$\alpha_v\beta_5$ (P1F6) Sepharose. Sepharose was prepared by binding 2 mg mAb to 1 ml cyanogen bromide–activated Sepharose (Pharmacia, Uppsala, Sweden) as recommended by the manufacturer. The affinity Sepharose was washed with 10 mM Tris-HCl (pH 8.0)/0.1% Tween-20 and 150 mM NaCl. Bound protein was eluted by incubation for 10 min at 65°C with nonreducing SDS sample buffer (Laemmli, 1970). Equivalent fractions of the total sample were electophoresed on 7.5% SDS-PAGE, transferred to Immobilon P (Millipore Corp.), and reacted with anti-β_3 mAb 7G2. Detection was by enhanced chemiluminesence according to the manufacturer's recommendations (ECL; Amersham Corp., Arlington Heights, IL).

Results

Vn-Bead Binding Is Deficient in OV10, But Can Be Restored by IAP Transfection

To analyze the structure–function relationships in IAP, we isolated an IAP-deficient clone, OV10, from the ovarian carcinoma cell line OVM1 (see Materials and Methods). OV10 cells express large amounts of β_1 and α_5 (not shown), a moderate amount of α_v and β_5, and a small amount of β_3 (Table I). When assayed for Vn-bead binding, OV10 cells showed attachment indices only marginally above those seen with beads coated with HSA. However, transfectants expressing IAP-2 (Fig. 1), the predominant form of IAP in myeloid cells, showed a markedly enhanced capacity to bind Vn-beads (Fig. 2 *A*). Binding was increased with increasing Vn density on the bead, but it remained IAP dependent up to saturating Vn concentrations (~12.5 μg/ml). The IAP-mediated enhancement of Vn-bead binding was completely reversed by the functional anti-IAP mAb B6H12 (Fig. 2 *A*). The IAP dependence was Vn specific, as binding to fibronectin (Fn)–opsonized beads was independent of IAP and unaffected by the presence of anti-IAP mAb B6H12 (Fig. 2 *B*). Vn-bead binding was entirely dependent on $\alpha_v\beta_3$ and $\alpha_v\beta_5$, as shown by its sensitivity to anti-β_3 mAb 7G2 (Fig. 2 *D*) and anti-$\alpha_v\beta_5$ mAb P1F6 (Fig. 2 *C*), and was independent of β_1 integrins, as shown by resistance to inhibition by anti-β_1 mAb P4C10 (Fig. 2 *C*). In contrast, Fn-bead binding was almost completely inhibited by P4C10, but unaffected by 7G2 (Fig. 2 *B*). Anti-IAP mAb 2D3 binds IAP with similar affinity as B6H12, but it

Table I. Mean Fluorescence of OV10 Transfectants in Flow Cytometry

Antibody Antigen		Mean fluorescence*						
Name‡	Plasmid§	6F2 (control)	B6H12 IAP	AP3	P1F6 $\alpha_v\beta_5$	L230 αv	OKT4A CD4	W6/32 MHC
—	—	0.50 ± 0.06	0.53 ± 0.04	0.64 ± 0.05	1.92 ± 0.29	3.42 ± 0.14	0.99 ± 0.11	12.17 ± 0.70
vector	pIAP58	0.73 ± 0.05	0.77 ± 0.01	0.83 ± 0.01	2.12 ± 0.56	3.99 ± 0.55	ND	30.15 ± 5.13
IAP-1	pIAP71	0.64 ± 0.07	1.71 ± 0.19	0.66 ± 0.05	2.14 ± 0.47	3.16 ± 0.28	ND	13.77 ± 2.23
IAP-2	pIAP45	0.74 ± 0.05	7.97 ± 0.54	0.90 ± 0.08	3.02 ± 0.69	4.69 ± 0.28	ND	22.80 ± 4.16
IAP-3	pIAP131	0.61 ± 0.04	2.82 ± 0.24	0.64 ± 0.04	2.04 ± 0.49	3.17 ± 0.31	ND	11.84 ± 2.39
IAP-4	pIAP120	0.79 ± 0.13	9.40 ± 0.99	0.77 ± 0.04	2.52 ± 0.26	4.90 ± 0.82	ND	23.50 ± 5.87
IAP-CD4	pIAP147	0.75 ± 0.00	0.68 ± 0.02	0.82 ± 0.03	2.18 ± 0.07	3.92 ± 0.12	3.10 ± 0.08	27.75 ± 0.39
IAP-GPI	pIAP148	0.66 ± 0.03	7.64 ± 0.30	0.73 ± 0.06	2.49 ± 0.40	3.57 ± 0.21	ND	20.80 ± 4.70
IAP-2(hi)	pIAP315	0.62 ± 0.07	36.93 ± 0.81	0.66 ± 0.05	2.32 ± 0.15	4.45 ± 0.16	ND	20.03 ± 1.47
IAP-TM	pIAP323	0.57 ± 0.05	11.68 ± 1.42	0.64 ± 0.04	2.72 ± 0.12	3.49 ± 0.12	ND	13.43 ± 0.80
β_3/vector	pIAP164 + 58	0.78 ± 0.08	0.82 ± 0.09	4.18 ± 1.86	1.54 ± 0.24	10.42 ± 0.36	ND	20.80 ± 4.70
β_3/IAP-2	pIAP164 + 45	0.80 ± 0.05	3.77 ± 0.13	7.01 ± 0.42	1.95 ± 0.32	12.53 ± 0.41	ND	17.73 ± 1.48
β_3/IAP-GPI‖	pIAP164 + 148	0.70 ± 0.05	6.06 ± 0.31	4.29 ± 0.10	1.89 ± 0.36	7.70 ± 0.28	ND	20.03 ± 1.47

*Mean and standard error from two to three determinations with saturating amounts of antibody are shown. Multiple assays throughout this study gave similar relative results. In all cases, the cell populations yielded narrow single peaks, except for IAP-2, IAP-GPI, and IAP-2(hi) where a small population (<10%) of low positive cells could be seen with anti-IAP, and β_3/vector where a small population (<10%) of cells could be seen with slightly higher staining with AP3 and L230. The murine IAP-2 expressing clone (mIAP) was not assayed in this experiment. In separate experiments, integrin expression on mIAP was not different from untransfected or vector transfected OV10 (— and *vector*, respectively).
‡The name given is that used in all of the figures and the text. For the clone name, see Materials and Methods.
§The plasmid used to transfect the OV10 parental cell line. Where two plasmids are listed, the first plasmid was transfected into OV10, a clone selected, and this clone was then used as a parent of all transfectants harboring this plasmid.
‖The IAP-GPI clone shown is 148A10. IAP expression of clone 148C11 is similar, and that of clone 148D12 is ~ 50% higher (not shown).
MHC, major histocompatibility complex class I antigen.

has been shown to be nonfunctional in assays of Vn-bead binding and other IAP-dependent integrin functions (Lindberg et al., 1993). This was also true in our transfection system, where mAb 2D3 did not inhibit Vn-bead binding of IAP transfectants (Fig. 2 *D*). Vn-bead binding was also high in OV10 expressing murine IAP, showing that the IAP effect on integrin function is not species specific (Fig. 2 *E*). This result also verified that the effect of anti-IAP mAb B6H12 is specific, since this mAb has no effect on Vn-bead binding by the murine IAP expressors.

IAP function has been associated with $\alpha_v\beta_3$ rather than $\alpha_v\beta_5$. To determine if this was true in OV10, we tested the effect of anti-$\alpha_v\beta_5$ mAb P1F6 on Vn- and Fn-bead binding. P1F6 completely inhibited Vn-bead binding in a manner similar to anti-β_3 mAb 7G2 (Fig. 2 *C*). Surprisingly, testing multiple preparations from several sources, we consistently found inhibition of Fn-bead binding by P1F6 as well (Fig. 2 *B*). This suggests that P1F6 ligation of $\alpha_v\beta_5$ may affect the function of multiple OV10 integrins, perhaps through "integrin cross talk" (Blystone et al., 1994, 1995). Thus, our data indicate that expression of IAP specifically and markedly enhances Vn-bead binding, but we cannot determine the relative contributions of $\alpha_v\beta_3$ and $\alpha_v\beta_5$.

Adhesion to a Vn-coated Surface Is IAP Independent

To investigate the role of IAP in adhesion to a Vn-coated surface, we adhered different transfectants to microtiter plate wells coated with different concentrations of Vn (1 ng/ml to 10 μg/ml) for 60 min, using the same conditions as for the Vn-bead binding. Adhesion was maximal at a coating concentration of 100 ng/ml Vn, and only marginally above background at 3 ng/ml (not shown). Anti-β_3 7G2 does not inhibit adhesion in other clearly $\alpha_v\beta_3$-dependent systems, and it failed to do so here as well. Therefore, anti-α_v mAb L230 was used in combination with anti-$\alpha_v\beta_5$ mAb P1F6 to dissect integrin dependence. At a Vn concentration of 50 ng/ml, binding was inhibited completely by L230 and almost completely by P1F6. Only minimal differences in binding between IAP-positive and IAP-negative cells were seen (Fig. 3), which correlated with small differences in $\alpha_v\beta_3$ and $\alpha_v\beta_5$ expression (Table I). OV10 expressing high levels of β_3 from transfected β_3 cDNA (β_3/vector and β_3/IAP-2) maintained significant binding in the presence of 10 μg/ml anti-$\alpha_v\beta_5$ mAb P1F6. This suggests that binding under these conditions was mainly $\alpha_v\beta_5$ mediated in the low β_3 cells (vector and IAP-2) and mediated by both α_v integrins in the high β_3 expressors. Both in the presence and absence of P1F6, there was no effect of anti-IAP B6H12 even at 150 μg/ml (Fig. 3; not shown). Thus, under these conditions, IAP is uninvolved either in β_1 integrin–dependent binding of particles coated with Fn or in adhesion to a Vn-coated surface.

The IAP Cytoplasmic Domain Is Irrelevant for Vn-Bead Binding

IAP exists as four different forms generated by alternative splicing that differ only in their carboxy-terminal cytoplasmic extensions. These forms are called IAP-1, IAP-2, IAP-3, and IAP-4 (Fig. 1), in order of increasing cytoplasmic tail length (Reinhold et al., 1995). While IAP is ubiquitously

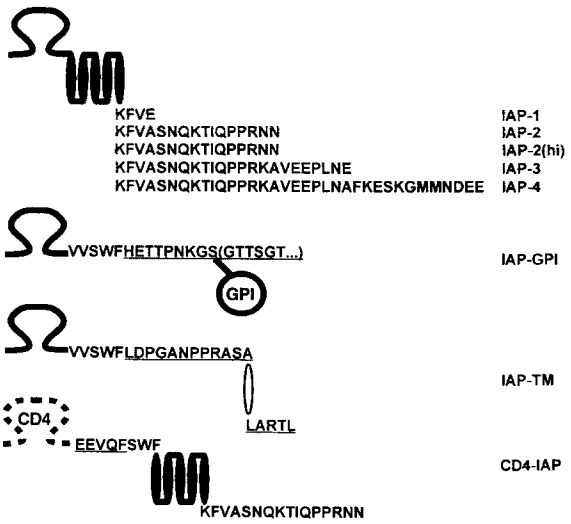

Figure 1. Predicted structure of IAP variants used. Amino acids are shown in single-letter amino acid code or as lines. Ovals represent membrane-spanning segments, and Ω denotes Ig domains. IAP-derived segments are shown as solid lines, ovals, and letters without underlining, while other segments are shown as broken lines (the CD4 IgV_1 domain), open ovals (the CD7 membrane segment), or underlined letters (sequences derived from CD4, CD7, or created in the fusion). The GPI anchor is shown as a circle connected to the serine residue to which the GPI anchor is linked. Residues shown within parentheses are removed as the GPI anchor is added. IAP-1, IAP-2, IAP-3, and IAP-4 correspond to naturally occurring splice variants of IAP. The expression of the correct tail has been verified for forms to which specific antisera have been raised (IAP-2 and IAP-4). IAP-2 and IAP-2(hi) differ only in the level of expression and the expression vector used. Murine IAP (mIAP) has the murine IAP-2 tail (not shown).

expressed, the alternative splicing is under strict cell type–specific control, leading to the almost exclusive expression of IAP-2 in myeloid cells and endothelium, and virtually exclusive expression of IAP-4 in neuronal tissue (Reinhold et al., 1995). To determine the role of the IAP cytoplasmic tail in Vn-bead binding, we used transfectants expressing the different splice forms of IAP in the bead binding assay. As shown in Fig. 2, *C* and *D*, expression of any of the four forms of IAP in OV10 led to enhancement of Vn-bead binding. This included IAP-1, which has only

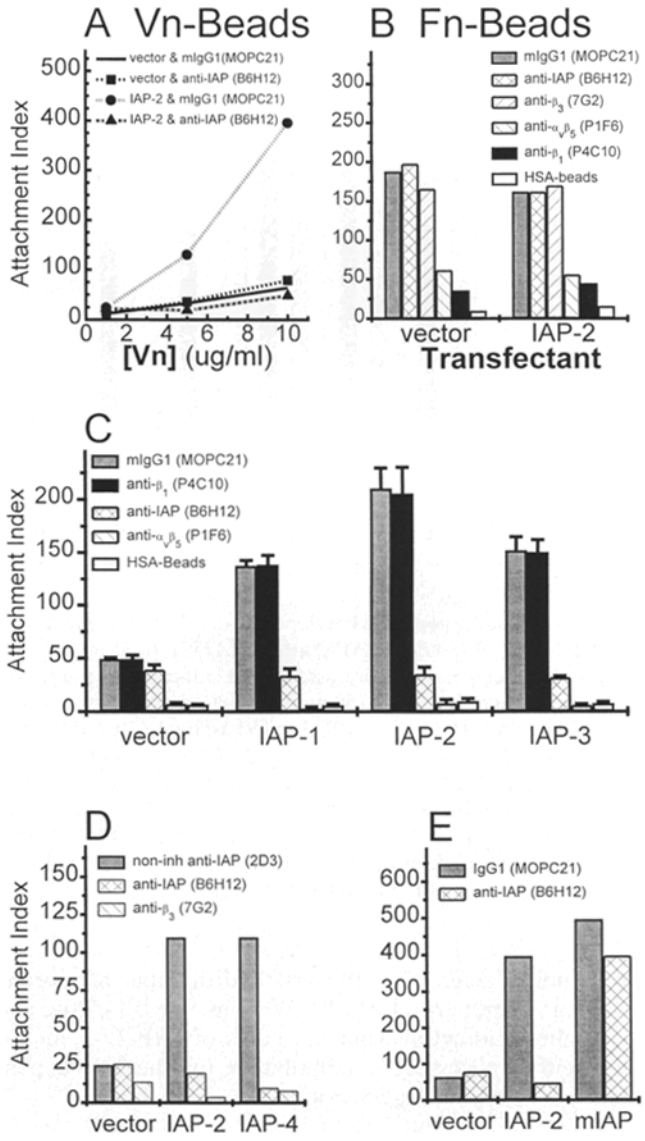

Figure 2. Efficient binding of vitronectin-coated but not fibronectin-coated particles is dependent on IAP. (*A*) OV10 transfected with vector alone (*vector*) or an IAP-2 expression construct (*IAP-2*) were assayed for Vn-bead binding, expressed as beads bound per 100 cells (*Attachment Index*). Before the assay, cells were preincubated for 20 min with the indicated mAbs (40 μg/ml), followed by two washes. Vn-beads prepared in different concentrations of vitronectin were used. Increasing the Vn concentration increased specific binding, but binding remained IAP dependent and B6H12 inhibitable. All binding was sensitive to anti-β_3 mAb 7G2 (not shown). (*B*) The experiment was performed as in *A*, except that beads were coated with 10 μg/ml fibronectin. IAP expression, anti-IAP mAbs B6H12, and anti-β_3 mAb 7G2 were all without effect (40 μg/ml), whereas anti-β_1 mAb P4C10 (1:50 dilution of ascites) inhibited binding. Surprisingly, anti-$\alpha_v\beta_5$ mAb P1F6 (40 μg/ml) inhibited binding to an extent comparable to anti-β_1 mAb P4C10 (see text). (*C*) OV10 transfected with vector alone (*vector*) or constructs encoding IAP alternative splice forms with successively longer cytoplasmic tails (*IAP-1*, *IAP-2*, *IAP-3*) were grown in Labtek chambers, and binding of Vn- or HSA-coated latex beads was assayed as in *A*. All three forms of IAP conferred the Vn-bead binding phenotype, which is sensitive to inhibition by anti-IAP mAb B6H12. Vn-bead binding was inhibited by anti-$\alpha_v\beta_5$ mAb P1F6, whereas anti-β_1 mAb P4C10 was without effect. Data are mean +SEM of three experiments performed under identical conditions. (*D*) Transfectants expressing the longest form of IAP (*IAP-4*) showed enhanced bead binding inhibited by anti-IAP mAb B6H12, whereas the nonfunctional anti-IAP mAb 2D3 had no effect. In all cases, Vn-bead binding was completely inhibited by anti-β_3 mAb 7G2. (*E*) OV10 transfected with vector alone, or constructs encoding human IAP-2 (*IAP-2*) or murine IAP-2 (*mIAP*) were assayed for Vn-bead binding. Both human and murine IAP mediated the enhancement of Vn-bead binding. Anti-IAP mAb B6H12 does not bind murine IAP. While it inhibited Vn-bead binding mediated by human IAP, it had no effect on binding mediated by murine IAP.

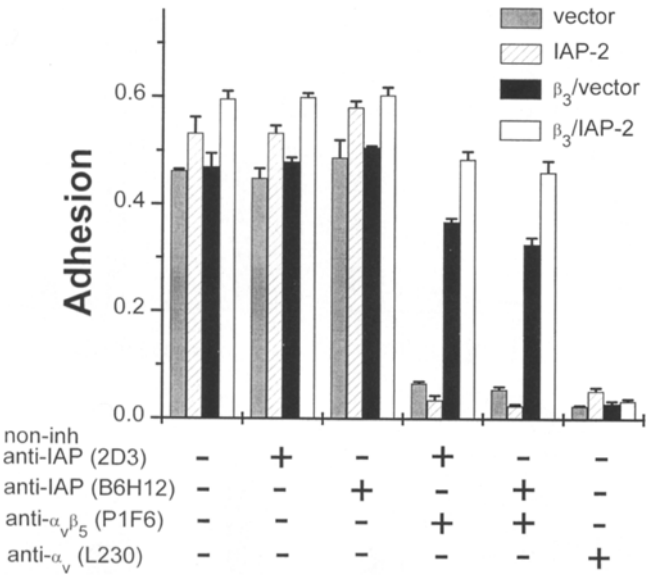

Figure 3. Vn adhesion is IAP independent. OV10 overexpressing IAP-2 and β_3 (*β_3/IAP-2*), IAP-2 alone (*IAP-2*), β_3 alone (*β_3/vector*), or neither (*vector*) were assayed for adhesion to microtiter plate wells coated with Vn (50 ng/ml) in the presence or absence of various mAbs (B6H12 and 2D3 at 150 μg/ml, L230 and P1F6 at 40 μg/ml). Maximal adhesion was 70–80%, and background was 0–2%. Means + SEM for triplicate wells from a representative experiment are shown. Experiments varying the Vn-coating concentration (1 ng/ml to 10 μg/ml) or incubation time (15–120 min), or the anti-IAP concentration (10 μg/ml to 150 μg/ml), failed to show any effect of IAP on the level of adhesion.

four amino acids after the last hydrophobic membrane segment (Lindberg et al., 1993). Thus, the 13–, 20–, and 32–amino acid cytoplasmic segments of IAP-2, -3, and -4 are neither necessary nor inhibitory for the IAP-dependent Vn-bead binding phenotype.

The IAP IgV Domain on a GPI Anchor Is Sufficient to Mediate the IAP Effect on Vn-Bead Binding

We next sought to determine the roles for the IAP extracellular and multiply membrane-spanning domains in Vn-bead binding. For this purpose, we made a construct encoding the IAP IgV domain fused to the human DAF GPI anchor signal (IAP–GPI), as well as the "inverse" construct encoding the human CD4 IgV_1 domain fused to the IAP-2 membrane and cytoplasmic domains (CD4–IAP) (Fig. 1). Clones of the corresponding transfectants expressed the recombinant proteins (Table I). Surprisingly, IAP–GPI enhanced Vn-bead binding, while CD4–IAP failed do so (Fig. 4 *A*). To confirm this unexpected finding, two additional transfectant clones of IAP–GPI were tested

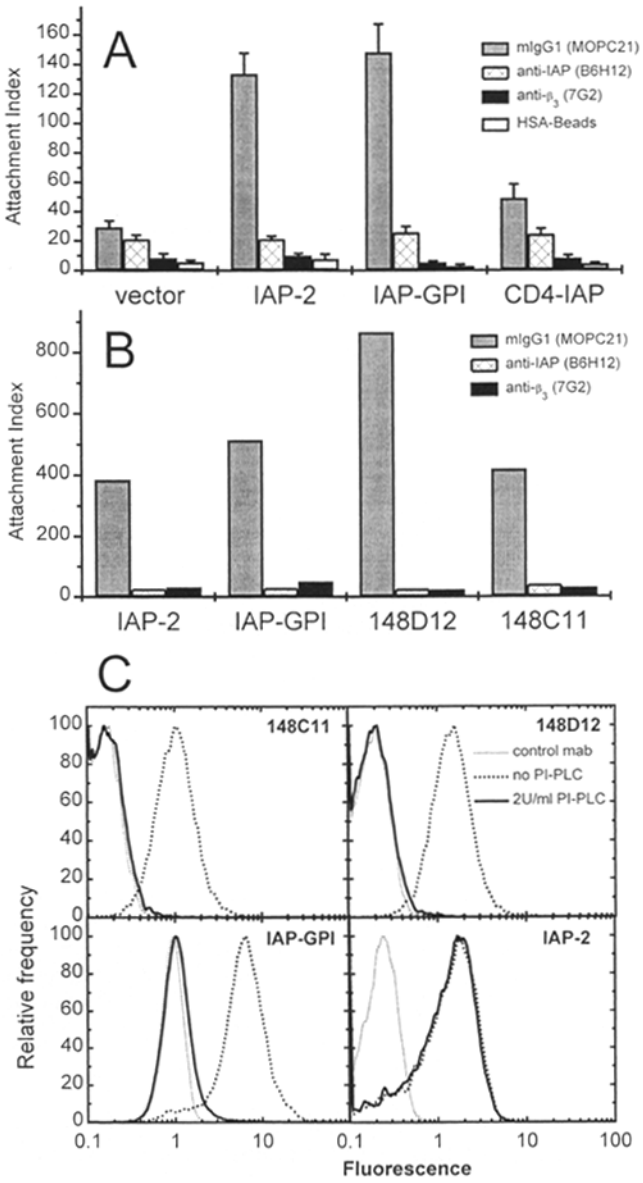

diated Vn-bead binding, suggesting that the IAP IgV domain is sufficient to complement the bead binding phenotype, and that the membrane and cytoplasmic domains are dispensable for this function. Data are mean + SEM of three experiments performed under identical conditions. (*B*) Another two independent IAP–GPI transfectants (*148D12* and *148C11*) were compared to IAP-2 and the original IAP-GPI clone (*IAP-GPI*) with similar results (representative of two experiments). (*C*) OV10 clones expressing IAP-GPI (*IAP-GPI*, *148C11*, *148D12*) and a control clone expressing IAP-2 were trypsinized and incubated for 1 h at 37°C in complete medium with 2 mM EDTA with or without 0. 2 U/ml PI-PLC, as described in Materials and Methods. After the digestion, cells were washed and stained with anti-IAP mAb 2D3 (no PI-PLC and 2 U/ml PI-PLC) followed by FITC-goat anti–mouse IgG and analysis by flow cytometry. As a negative control, untreated cells were stained with mAb 6F2 (*control mAb*). PI-PLC–treated cells gave identical reactivity with the control mAb and are therefore not shown. The PI-PLC treatment completely removed surface IAP reactivity from the IAP-GPI clones, whereas it had no effect on wild-type IAP, showing that the clones indeed expressed the expected IAP form (representative of two experiments). Data obtained using anti-IAP mAb 1F7 were identical (not shown).

Figure 4. The IAP IgV domain is sufficient to mediate vitronectin bead binding. (*A*) Vitronectin- and HSA-coated latex particle binding were assayed as in Fig. 2. OV10 cells were transfected with vector alone (*vector*), wild-type IAP (*IAP-2*), a construct encoding the IAP IgV domain linked to a DAF GPI signal (*IAP–GPI*), or the CD4-IgV_1 domain linked to the IAP-2 membrane and cytoplasmic domain (*CD4–IAP*). Surprisingly, IAP–GPI me-

for Vn-bead binding, yielding similar results (Fig. 4 *B*). Furthermore, we confirmed that IAP–GPI was in fact GPI linked by demonstrating that essentially all anti-IAP reactivity could be removed from the surface of IAP–GPI by PI-PLC, whereas expression of wild-type IAP-2 was unaffected by this enzyme (Fig. 4 *C*). Thus, the GPI-anchored IAP IgV domain is sufficient for the restoration of Vn-bead binding to IAP-deficient cells.

The IAP IgV Domain Functions Irrespective of the Nature of the Domain Anchoring It to the Membrane

GPI-anchored proteins exist in specialized membrane domains in which they are associated with intracellular src kinases (Brown, 1993). Cross-linking of several GPI-linked proteins leads to kinase activation (Brown, 1993). It is therefore theoretically possible that the IAP multiply membrane-spanning domain functions in a manner that can be duplicated by these special properties of the GPI anchor. To exclude this possibility, we generated cells expressing the IAP-IgV domain linked to the single transmembrane segment of human CD7 (IAP–TM) (Fig. 1). As shown in Fig. 5 *A*, this construct enhanced Vn-bead binding as well as IAP-2 and IAP–GPI, showing that the membrane-anchored IAP-IgV domain suffices for this phenotype, irrespective of the exact nature of the membrane anchor.

Increases in Either IAP or $\alpha_v\beta_3$ Expression Lead to Increased Vn-Bead Binding

We observed that the extent of Vn-bead binding correlated with the level of IAP expression regardless of splice form. This suggested that IAP expression was limiting to Vn-bead binding. To test this hypothesis, we made a construct encoding IAP-2 using a more efficient promoter (see Materials and Methods). A transfectant of this construct (IAP-2[hi]) expressed IAP at significantly higher levels than the control clone (IAP-2) (Table I) and bound Vn-beads at a significantly higher level than the IAP-2 construct (attachment index of 373 vs 181) (Fig. 5 *B*). Thus, the extent of bead binding correlated with IAP expression.

It was surprising that Vn-bead binding was inhibited by anti-β_3 mAb 7G2, even though OV10 expresses only minimal levels of integrin $\alpha_v\beta_3$ (Table I). To investigate this further, and to test the hypothesis that IAP dependence could be overcome by increased surface expression of the integrin, we derived a series of clones with high $\alpha_v\beta_3$ expression by transfection with β_3-encoding constructs (Materials and Methods). Even with high expression of the $\alpha_v\beta_3$, Vn-bead binding was markedly enhanced by IAP (Fig. 5 *C*). Clones overexpressing both the integrin and IAP (β_3/IAP-2) bound Vn-beads to a much greater extent than even the IAP-2(hi) clone (Fig. 5 *B*), although they had significantly lower IAP surface expression than IAP-2(hi) (3.77 ± 0.13 vs 36.93 ± 0.81; see Table I). Thus, both $\alpha_v\beta_3$ expression and IAP expression are limiting for Vn-bead binding by OV10. In the $\alpha_v\beta_3$-overexpressing clones, the membrane-anchored IAP IgV domain alone was still sufficient to restore Vn-bead binding, since expression of IAP–GPI was as efficient as IAP-2 (Fig. 5 *C*; lower attachment indices in this experiment reflect the lower bead concentrations used in this experiment). As with the original OV10 IAP transfectants, the enhancement of Vn-bead binding in the $\alpha_v\beta_3$-overexpressing cells was completely reversed by anti-IAP mAb B6H12 and completely inhibited by anti-β_3 mAb 7G2. Despite overexpression of $\alpha_v\beta_3$,

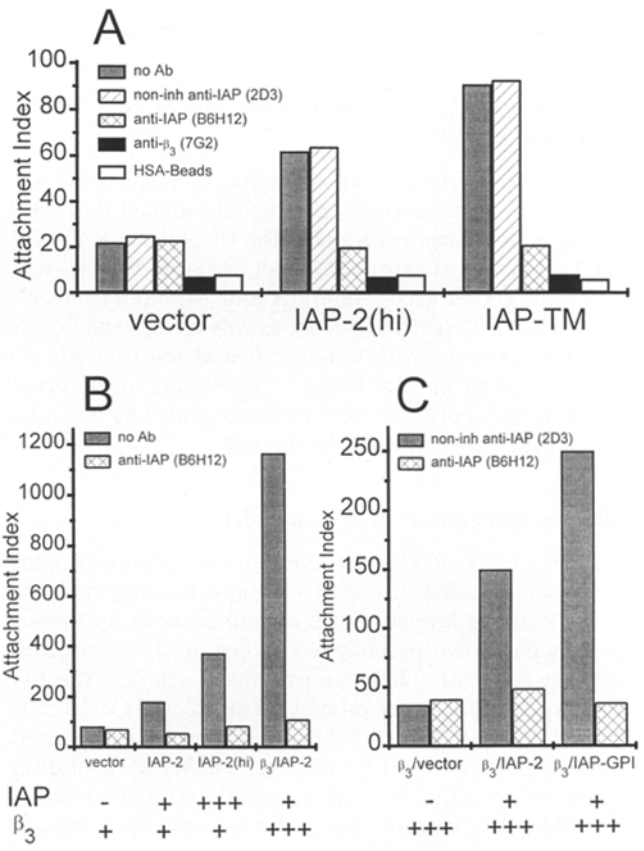

Figure 5. Bead binding is supported by the IAP IgV domain irrespective of membrane anchor and related to the level of both IAP and $\alpha_v\beta_3$ expression. Vn-bead binding was assayed as in Fig. 2, using OV10 transfected with vector alone (*vector*), a high level IAP-2 expression construct (*IAP–2[hi]*), or a construct expressing IAP IgV fused to the human CD7 transmembrane segment (*IAP–TM*). IAP–TM mediated enhancement of Vn-bead binding, showing that the nature of the membrane anchor is unimportant (IAP membrane domain vs GPI anchor vs CD7 membrane segment) in this system. (*B*) Vn-bead binding was assayed with OV10 transfected with vector alone (*vector*), the clone expressing IAP-2 (*IAP-2*), a clone expressing approximately fourfold higher levels of IAP-2 (*IAP-2[hi]*), or a transfectant overexpressing both IAP-2 and integrin $\alpha_v\beta_3$ (β_3/*IAP-2*). Attachment indices obtained in the presence of 40 μg/ml anti-β_3 mAb 7G2 were 9, 11, 13, and 22, respectively, and those obtained with HSA beads were 1, 2, 1, and 5, respectively. Increases in IAP expression increased Vn-bead binding, as did increased $\alpha_v\beta_3$ expression. (*C*) A transfectant expressing high levels of $\alpha_v\beta_3$ was generated and retransfected with vector alone (β_3/*vector*), or expression constructs for IAP-2 (β_3/*IAP-2*) or IAP–GPI (β_3/*IAP–GPI*). In the presence of 40 μg/ml 7G2, attachment indices were 2, 5, and 5, respectively. With HSA beads, they were ≤2. As all these $\alpha_v\beta_3$ overexpressors showed markedly enhanced binding (see *B*), fewer beads were used in the assay, to arrive at countable levels of Vn-bead binding (see Materials and Methods). Despite the higher level of $\alpha_v\beta_3$ expression, Vn-bead binding is still IAP dependent and can be mediated by the GPI-anchored IAP-IgV domain.

anti-$\alpha_v\beta_5$ mAb P1F6 also completely inhibited Vn-bead binding (Fig. 6).

Induction of β_3 Ligand–induced Binding Sites Is Not Influenced by IAP

To determine if IAP alters the affinity state of $\alpha_v\beta_3$, we determined the generation of the ligand-induced β_3 LIBS1 epitope by increasing concentration of peptide KYAVTG**RGDS** on OV10 expressing high amounts of $\alpha_v\beta_3$ with or without IAP-2 (see Materials and Methods). Over a range of 1–1,000 μM ligand, there was clear induction of the LIBS1 epitope, with a higher ligand sensitivity in 0.1 mM $MnCl_2$ than in 5 mM $MgCl_2$. However, we observed no difference between IAP-positive and IAP-negative cells in these experiments (not shown).

Coimmunoprecipitation of β_3 and IAP

The dependence of Vn-bead binding on the plasma membrane concentration of both IAP and $\alpha_v\beta_3$ suggested that the relevant binding structure contained both molecules, as has been shown previously (Brown et al., 1990; Zhou and Brown, 1993). Thus, we examined whether the two proteins could be coprecipitated in transfected OV10 cells. When either IAP-2 or IAP–GPI was immunoprecipitated, coprecipitated β_3 could be detected by Western blotting (Fig. 7), showing that the $\alpha_v\beta_3$ association can be mediated by the IAP IgV domain alone. No β_3 was coprecipitated with $\alpha_v\beta_5$. Coprecipitated β_3 was a small minority of total

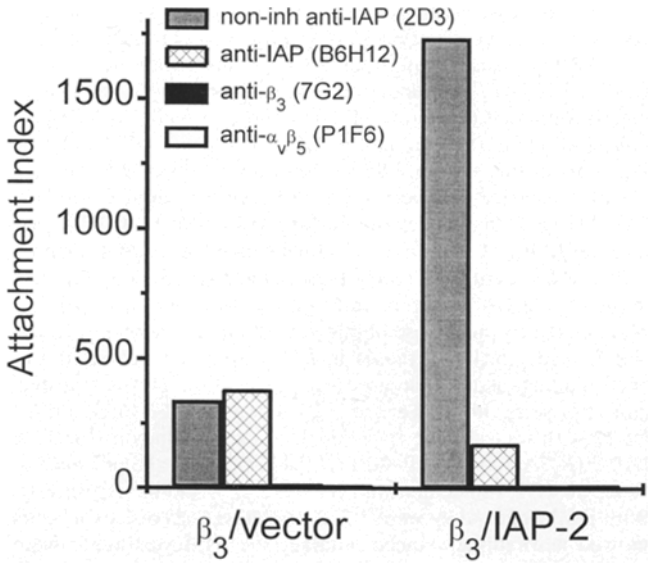

Figure 6. Both anti-β_3 and anti-$\alpha_v\beta_5$ inhibit Vn-bead binding even in $\alpha_v\beta_3$ overexpressors. OV10 transfectants expressing high levels of $\alpha_v\beta_3$ alone (*β_3/vector*) or IAP-2, and high levels of $\alpha_v\beta_3$ (*β_3/IAP-2*) were assayed for Vn-bead binding. Preincubation with anti-IAP mAb B6H12 inhibits the increase in bead binding obtained by IAP-2 expression, whereas noninhibitory anti-IAP mAb 2D3 has no effect. Both anti-β_3 mAb 7G2 and anti-$\alpha_v\beta_5$ mAb P1F6 inhibited Vn-bead binding completely. Attachment indices with HSA beads were ≤5. Absolute attachment indices are higher than in Fig. 5 *C* as a result of the use of higher amounts of Vn-beads (see Materials and Methods).

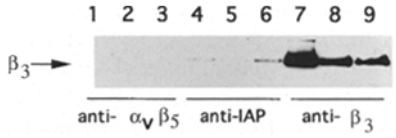

Figure 7. Both IAP-2 and IAP–GPI associate with β_3 integrin. Cell extracts in 100 mM octyl-glucoside were prepared from transfectants overexpressing $\alpha_v\beta_3$ and IAP-2 (lanes *1*, *4*, and *7*), $\alpha_v\beta_3$ alone, (lanes *2*, *5*, and *8*), or $\alpha_v\beta_3$ and IAP–GPI (lanes *3*, *6*, and *9*) and immunoprecipitated with anti-$\alpha_v\beta_5$ mAb P1F6, anti-IAP mAb 2D3, or anti-β_3 mAb 7G2. Immunoprecipitates were separated by nonreducing SDS-PAGE, transferred to Immobilon P, and immunoblotted with anti-β_3 mAb 7G2. Peroxidase-conjugated anti–mouse IgG was used as a secondary antibody, followed by detection with enhanced chemiluminesence. A reactive band migrating at the β_3 position (~95 kD) can be seen in both the IAP-2 and IAP–GPI transfectants (lanes *4* and *6*), but is absent in the IAP-deficient control (lane *5*). No β_3 was coprecipitated with the control antibody P1F6, whereas anti-β_3 mAb 7G2 could immmunoprecipitate the antigen from all three cell types. Thus, both IAP variants associate with β_3 integrin.

β_3, suggesting that the majority of both IAP and $\alpha_v\beta_3$ was not in a stable complex.

Discussion

Antibody to integrin-associated protein (IAP/CD47) has been shown to affect a large number of cell functions associated with $\alpha_v\beta_3$ and $\alpha_v\beta_3$-like integrins, such as Vn-bead binding, RGD activation of Fc-receptor–mediated phagocytosis, chemotaxis, and oxidative burst, as well as PMN migration through epithelial or endothelial barriers (Parkos et al., 1991, 1996; Cooper et al., 1995; Gresham et al., 1992; Senior et al., 1992). Because of the ubiquity of IAP expression, it has been difficult to determine if the effects of anti-IAP mAb were to inhibit IAP function, or if mAb binding to IAP generated a negative signal that then inhibited function. Indeed, the transfection of human IAP into CHO cells expressing hamster IAP made Vn-bead binding sensitive to the anti-human IAP mAb B6H12, raising the possibility that the antibody generated a signal that specifically regulated α_v integrin function (Lindberg et al., 1993). In this paper, we have directly tested whether or not IAP is necessary for Vn-bead binding by α_v integrins. We have shown that a cell line lacking IAP fails to bind Vn-beads and that expression of IAP on these cells confers the ability to bind Vn-coated particles. Increased integrin expression led to increased binding, but failed to obviate the IAP requirement. Thus, the phenotype of IAP-deficient cells is similar to that of anti-IAP–treated, IAP-expressing cells. The requirement for IAP does not reflect direct binding of Vn-beads by IAP, since in all cases it is inhibited completely by anti-β_3 and $\alpha_v\beta_5$ mAbs. Expression of IAP does not influence β_1 integrin bead binding, since $\alpha_5\beta_1$ integrin–mediated binding of Fn-beads is unaffected by the absence of IAP.

In requiring IAP, Vn-bead binding differs from adhesion to a Vn-coated surface, which is IAP independent. Similarly, α_v-dependent spreading of endothelial cells on Vn is IAP independent, whereas the concomitant rise in intracellular calcium concentration can be inhibited by

anti-IAP mAbs (Schwartz et al., 1993). A difference in Fn-bead binding and adhesion to a Fn-coated surface has been described for K562 cells, which was attributed to the requirement for a high affinity $\alpha_5\beta_1$ in Fn-bead binding (Blystone et al., 1994). Possibly, IAP is necessary for a higher avidity of $\alpha_v\beta_3$, which might be required for Vn-bead binding. Whether this reflects a dependence on IAP for generation of high affinity $\alpha_v\beta_3$ or another mechanism for creating increased avidity, such as receptor clustering or altered receptor interaction with the cytoskeleton, is unclear. However, while RGD peptide induced the activation-dependent LIBS1 epitope on $\alpha_v\beta_3$-overexpressing OV10, this was independent of IAP expression. Whatever the mechanism, these studies clearly demonstrate an important distinction between bead binding and adhesion. Thus, studies using bead binding as a model for adhesion to a surface (Miyamoto et al., 1995*a*,*b*) need to be interpreted with some caution.

The extent of Vn-bead binding is dependent on the levels of both IAP and $\alpha_v\beta_3$ expression, but even increasing $\alpha_v\beta_3$ expression 10-fold did not make bead binding IAP independent. Previous work in K562 cells has shown that Vn-bead binding also requires expression of α_v integrins (Blystone et al., 1994). Since Vn-bead binding is sensitive to the concentrations of both IAP and $\alpha_v\beta_3$ in the cell membrane, it is likely that bead binding requires a physical complex between IAP and the integrin. As previously shown for platelets (Brown et al., 1990), integrin β_3 coimmunoprecipitates with IAP in OV10 transfectants. However, under the conditions of the assay, most IAP on the cell surface is not associated with β_3 integrin, and most $\alpha_v\beta_3$ is not associated with IAP. Using the mild detergent conditions required to show coprecipitation, IAP is relatively poorly solubilized, whereas harsher conditions disrupt IAP–integrin association. It is clear, since IAP can be expressed on cells in the absence of α_v integrins (Blystone et al., 1994), and α_v integrins can be expressed without IAP in OV10, that transport to the plasma membrane does not require complex formation between these proteins. Instead, the complex probably forms on the plasma membrane, presumably in equilibrium with free IAP and $\alpha_v\beta_3$. The complex has ligand-binding properties distinct from free $\alpha_v\beta_3$. A simple explanation for the requirement of IAP in α_v integrin bead binding would be that IAP is necessary for generation of the high affinity form of the integrin. However, we found no evidence for any IAP-dependent change in ligand affinity, using the display of the LIBS1 epitope as assay. This does not rule out the possibility that a small but functionally important subset of α_v integrin molecules are affinity regulated by IAP, but it is more likely that IAP acts in some other way to alter the function of α_v integrins. It will be interesting and important to determine which of the integrin's functions in migration, neovascularization, metastasis, etc. (Leavesley et al., 1992, 1993; Brooks et al., 1994; Filardo et al., 1995) are actually dependent on its association with IAP.

OV10 cells express much more $\alpha_v\beta_5$ than $\alpha_v\beta_3$ (Table I). Since Vn-bead binding is dependent on IAP, and on K562 cells (which express IAP), $\alpha_v\beta_5$ can bind Vn-beads in the absence of $\alpha_v\beta_3$ (Blystone et al., 1994), it is very likely that $\alpha_v\beta_5$ also interacts functionally with IAP. We could not coimmunoprecipitate IAP with $\alpha_v\beta_5$, but this may reflect only a slightly lower interaction between the two molecules in detergent solution than between IAP and $\alpha_v\beta_3$. Both anti-β_3 mAb 7G2 and anti-$\alpha_v\beta_5$ mAb P1F6 completely inhibit Vn-bead binding regardless of the relative amounts of $\alpha_v\beta_3$ and $\alpha_v\beta_5$. Furthermore, P1F6 but not 7G2 blocked Fn-bead binding. In contrast, P1F6 had no effect on adhesion to Vn (Fig. 3) or Fn (not shown). While the basis of these effects of α_v integrin antibodies on bead binding is unknown, they may reflect interintegrin signaling (cross talk) (Blystone et al., 1994, 1995). Alternatively, inhibition may reflect clustering of several integrins at sites of cell–bead contact, with resulting steric inhibition of binding by either mAb. However, IAP would reasonably be expected to be present in such an aggregate, and a purely sterical inhibition is hard to reconcile with the lack of effect of the noninhibitory anti-IAP mAb 2D3.

The absence of IAP in OV10 cells allowed the first structure–function studies on IAP. These studies demonstrated that the amino-terminal IgV domain was necessary and sufficient for Vn-bead binding. The importance of the IgV domain of IAP for interaction with α_v integrins is intriguing because interactions between Ig family members and integrins are well-described mechanisms for cell–cell interaction in the immune system. ICAM-1 interaction with β_2 integrins (Diamond et al., 1991; Staunton et al., 1990), PECAM-1 with $\alpha_v\beta_3$ (Piali et al., 1995; Buckley et al., 1996), VCAM-1 with $\alpha_4\beta_1$(Elices et al., 1990), and MadCAM with $\alpha_4\beta_7$ (Berlin et al., 1993; Briskin et al., 1996) all have roles in transendothelial migration of leukocytes. In contrast to these cell–cell adhesive interactions, the IAP–integrin interaction must involve an IgV domain on the same cell as the integrin. IAP interaction with α_v integrins would represent an extension of the paradigm of Ig family–integrin binding to interactions between molecules on a single plasma membrane.

The cell type–specific expression of different cytoplasmic tail forms of IAP would suggest that this part of the molecule has a specific functional role. Also, the anti-IAP inhibitable inward calcium flux in endothelial cells spreading on Vn (Schwartz et al., 1993) makes the IAP multiply membrane-spanning domain a potential candidate for a channel. Surprisingly, both these parts of the IAP molecule are dispensable for Vn-bead binding in our transfection system. It is theoretically possible that a mutated form of IAP is expressed by OV10 and is able to interact with IAP–GPI and IAP–TM, reconstituting a functional but noncovalently associated IAP molecule. However, we have been unable to detect in OV10 any IAP message by reverse transcriptase–PCR, any IAP-2 or IAP-4 cytoplasmic tail by immunoblot or immunoprecipitation with specific antisera, or any IAP Ig immunoglobulin domain with monoclonal and polyclonal anti-IAP antibodies by immunoprecipitation or FACS® (not shown). This makes the existence of any mutant IAP protein in OV10 highly unlikely. More likely, while interaction with α_v integrins is mediated by the IgV domain, other, as yet undefined functions of IAP require these other domains.

Recently, IAP has been shown to be the receptor for the carboxy-terminal cell-binding domain of thrombospondin-1 (TS-1) (Gao et al., 1996). TS-1 is a 450-kD trimeric matrix protein that, in addition to the cell-binding domain, has several other cell- and matrix-interaction domains, includ-

ing a RGD sequence capable of ligating $\alpha_v\beta_3$. This suggests the possibility that the Vn used may contain small amounts of TS-1, and that this contaminant is responsible for the IAP effect on Vn-bead binding. However, binding of beads coated with synthetic RGD peptides and analogs is also inhibited by anti-IAP (Gresham et al., 1989, 1992; Brown et al., 1990), ruling out the possibility that TS-1 contamination of Vn is the reason for the IAP dependence.

In summary, this work is the first to show that any specific function of α_v requires IAP. Surprisingly, Vn-bead binding by α_v integrins, which is IAP dependent in OV10 cells, requires only a membrane-associated IAP IgV domain, and the IgV domain is sufficient to mediate coimmunoprecipitation of IAP with $\alpha_v\beta_3$. This suggests that the IAP–$\alpha_v\beta_3$ complex represents an extension of the integrin–Ig family adhesive interactions to molecules on a single plasma membrane for the purpose of modulating integrin function. The structural details and biological consequences of this modulation, as well as the functions of the more complex membrane-spanning and cytoplasmic domains of IAP, remain to be determined.

We thank Matthew Williams and Alexander Zheleznyak for excellent technical assistance, and Dr. Scott Blystone for critically reviewing this manuscript.

This research was funded grant GM38330 from the National Institutes of Health (to E.J. Brown), a Howard Hughes Physician-Scientist fellowship (to F.P. Lindberg), an Arthritis Investigator Award (to F.P. Lindberg), the Monsanto-Washington University Agreement (to E.J. Brown), and the Medical Research Service of the Department of Veterans Affairs (to H.D. Gresham).

Received for publication 17 May 1996 and in revised form 2 July 1996.

References

Berlin, C., E.L. Berg, M.J. Briskin, D.P. Andrew, P.J. Kilshaw, B. Holzmann, I.L. Weissman, A. Hamann, and E.C. Butcher. 1993. $\alpha_4\beta_7$ integrin mediates lymphocyte binding to the mucosal vascular addressin MAdCAM-1. *Cell.* 74:185.

Blystone, S.D., I.L. Graham, F.P. Lindberg, and E.J. Brown. 1994. Integrin $\alpha_v\beta_3$ differentially regulates adhesive and phagocytic functions of the fibronectin receptor $\alpha_5\beta_1$. *J. Cell Biol.* 127:1129–1137.

Blystone, S.D., F.P. Lindberg, S.E. LaFlamme, and E.J. Brown. 1995. Integrin β_3 cytoplasmic tail is necessary and sufficient for regulation of $\alpha_5\beta_1$ phagocytosis by $\alpha_v\beta_3$ and integrin-associated protein. *J. Cell Biol.* 130:745–754.

Briskin, M.J., L. Rott, and E.C. Butcher. 1996. Structural requirements for mucosal vascular addressin binding to its lymphocyte receptor $\alpha_4\beta_7$. Common themes among integrin-Ig family interactions. *J. Immunol.* 156:719–726.

Brooks, P.C., R.A. Clark, and D.A. Cheresh. 1994. Requirement of vascular integrin $\alpha_v\beta_3$ for angiogenesis. *Science (Wash. DC).* 264:569–571.

Brown, D. 1993. The tyrosine kinase connection: how GPI-anchored proteins activate T cells. *Curr. Opin. Immunol.* 5:349–354.

Brown, E.J., L. Hooper, T. Ho, and H.D. Gresham. 1990. Integrin-associated protein: a 50-kD plasma membrane antigen physically and functionally associated with integrins. *J. Cell Biol.* 111:2785–2794.

Buckley, C.D., R. Doyonnas, J.P. Newton, S.D. Blystone, E.J. Brown, S.M. Watt, and D.L. Simmons. 1996. Identification of $\alpha_v\beta_3$ as a heterotypic ligand for CD31/PECAM-1. *J. Cell Sci.* 109:437–445.

Campbell, I.G., P.S. Freemont, W. Foulkes, and J. Trowsdale. 1992. An ovarian tumor marker with homology to vaccinia virus contains an IgV-like region and multiple transmembrane domains. *Cancer Res.* 52:5416–5420.

Cooper, D., F.P. Lindberg, J.R. Gamble, E.J. Brown, and M.A. Vadas. 1995. The transendothelial migration of neutrophils involves integrin-associated protein (CD47). *Proc. Natl. Acad. Sci. USA.* 92:3978–3982.

Diamond, M.S., D.E. Staunton, S.D. Marlin, and T.A. Springer. 1991. Binding of the integrin Mac-1 (CD11b/CD18) to the third immunoglobulin-like domain of ICAM-1 (CD54) and its regulation by glycosylation. *Cell.* 65:961–971.

Elices, M.J., L. Osborn, Y. Takada, C. Crouse, S. Luhowskyj, M.E. Hemler, and R.R. Lobb. 1990. VCAM-1 on activated endothelium interacts with the leukocyte integrin VLA-4 at a site distinct from the VLA- 4/fibronectin binding site. *Cell.* 60:577–584.

Filardo, E.J., P.C. Brooks, S.L. Deming, C. Damsky, and D.A. Cheresh. 1995. Requirement of the NPXY motif in the integrin β_3 subunit cytoplasmic tail for melanoma cell migration in vitro and in vivo. *J. Cell Biol.* 130:441–450.

Frelinger, A.L., I. Cohen, E.F. Plow, M.A. Smith, J. Roberts, S.C. Lam, and M.H. Ginsberg. 1990. Selective inhibition of integrin function by antibodies specific for ligand-occupied receptor conformers. *J. Biol. Chem.* 265:6346–6352.

Gao, A.G., F.P. Lindberg, M.B. Finn, S.D. Blystone, and W.A. Frazier. 1996. Integrin-associated protein is a receptor for the C-terminal domain of thrombospondin. *J. Biol. Chem.* 271:21–24.

Gresham, H.D., J.L. Goodwin, P.M. Allen, D.C. Anderson, and E.J. Brown. 1989. A novel member of the integrin receptor family mediates Arg-Gly-Asp–stimulated neutrophil phagocytosis. *J. Cell Biol.* 108:1935–1943.

Gresham, H.D., S.P. Adams, and E.J. Brown. 1992. Ligand binding specificity of the leukocyte response integrin expressed by human neutrophils. *J. Biol. Chem.* 67:13895–13902.

Kolanus, W., C. Romeo, and B. Seed. 1993. T cell activation by clustered tyrosine kinases. *Cell.* 74:171–183.

Laemmli, U.K. 1970. Cleavage of structural proteins during the assembly of the head of bacteriophage T4. *Nature (Lond.).* 227:680–685.

Leavesley, D.I., G.D. Ferguson, E.A. Wayner, and D.A. Cheresh. 1992. Requirement of the integrin β_3 subunit for carcinoma cell spreading or migration on vitronectin and fibrinogen. *J. Cell Biol.* 117:1101–1107.

Leavesley, D.I., M.A. Schwartz, M. Rosenfeld, and D.A. Cheresh. 1993. Integrin β_1- and β_3-mediated endothelial cell migration is triggered through distinct signaling mechanisms. *J. Cell Biol.* 121:163–170.

Lindberg, F.P., H.D. Gresham, E. Schwarz, and E.J. Brown. 1993. Molecular cloning of integrin-associated protein: an immunoglobulin family member with multiple membrane-spanning domains implicated in α_v, β_3-dependent ligand binding. *J. Cell Biol.* 123:485–496.

Lindberg, F.P., D.M. Lublin, M.J. Telen, R.A. Veile, Y.E. Miller, H. Donis-Keller, and E.J. Brown. 1994. Rh-related antigen CD47 is the signal-transducer integrin-associated protein. *J. Biol. Chem.* 269:1567–1570.

Loftus, J.C., T.E. O'Toole, E.F. Plow, A. Glass, A.L. Frelinger, and M.H. Ginsberg. 1990. A β_3 integrin mutation abolishes ligand binding and alters divalent cation-dependent conformation. *Science (Wash. DC).* 249:915–918.

Mawby, W.J., C.H. Holmes, D.J. Anstee, F.A. Spring, and M.J. Tanner. 1994. Isolation and characterization of CD47 glycoprotein: a multispanning membrane protein which is the same as integrin-associated protein (IAP) and the ovarian tumour marker OA3. *Biochem. J.* 304:525–530.

Medof, M.E., D.M. Lublin, V.M. Holers, D.J. Ayers, R.R. Getty, J.F. Leykam, J.P. Atkinson, and M.L. Tykocinski. 1987. Cloning and characterization of cDNAs encoding the complete sequence of decay-accelerating factor of human complement. *Proc. Natl. Acad. Sci. USA.* 84:2007–2011.

Miyamoto, S., S.K. Akiyama, and K.M. Yamada. 1995*a*. Synergistic roles for receptor occupancy and aggregation in integrin transmembrane function. *Science (Wash. DC).* 267:883–885.

Miyamoto, S., H. Teramoto, O.A. Coso, J.S. Gutkind, P.D. Burbelo, S.K. Akiyama, and K.M. Yamada. 1995*b*. Integrin function: molecular hierarchies of cytoskeletal and signaling molecules. *J. Cell Biol.* 131:791–805.

Parkos, C.A., C. Delp, M.A. Arnaout, and J.L. Madara. 1991. Neutrophil migration across a cultured intestinal epithelium. Dependence on a CD11b/CD18-mediated event and enhanced efficiency in physiological direction. *J. Clin. Invest.* 88:1605–1612.

Parkos, C.A., S.P. Colgan, T.W. Liang, A. Nusrat, A.E. Bacarra, D.K. Carnes, and J.L. Madara. 1996. CD47 mediates post-adhesive events required for neutrophil migration across polarized intestinal epithelia. *J. Cell Biol.* 132: 437–450.

Piali, L., P. Hammel, C. Uherek, F. Bachmann, R.H. Gisler, D. Dunon, and B.A. Imhof. 1995. CD31/PECAM-1 is a ligand for $\alpha_v\beta_3$ integrin involved in adhesion of leukocytes to endothelium. *J. Cell Biol.* 130:451–460.

Reinhold, M.R., F.P. Lindberg, D. Plas, S. Reynolds, M.G. Peters, and E.J. Brown. 1995. In vivo expression of alternatively spliced forms of integrin-associated protein (CD47). *J. Cell Sci.* 108:3419–3425.

Rosales, C., H.D. Gresham, and E.J. Brown. 1992. Expression of the 50-kD integrin-associated protein on myeloid cells and erythrocytes. *J. Immunol.* 149: 2759–2764.

Sanger, F., S. Nicklen, and A.R. Coulson. 1977. DNA sequencing with chain-terminating inhibitors. *Proc. Natl. Acad. Sci. USA.* 74:5463–5467.

Schwartz, M.A., E.J. Brown, and B. Fazeli. 1993. A 50 kDa integrin-associated protein is required for integrin-regulated calcium entry in endothelial cells. *J. Biol. Chem.* 268:19931–19934.

Senior, R.M., H.D. Gresham, G.L. Griffin, E.J. Brown, and A.E. Chung. 1992. Entactin stimulates neutrophil adhesion and chemotaxis through interactions between its Arg-Gly-Asp (RGD) domain and the leukocyte response integrin. *J. Clin. Invest.* 90:2251–2257.

Staunton, D.E., M.L. Dustin, H.P. Erickson, and T.A. Springer. 1990. The arrangement of the Ig-like domains of ICAM-1 and the binding sites for LFA-1 and rhinovirus. *Cell.* 61:243–254.

Wayner, E.A., R.A. Orlando, and D.A. Cheresh. 1991. Integrins $\alpha_v\beta_3$ and $\alpha_v\beta_5$ contribute to cell attachment to vitronectin but differentially distribute on the cell surface. *J. Cell Biol.* 113:919–929.

Weinacker, A., A. Chen, M. Agrez, R.I. Cone, S. Nishimura, E. Wayner, R. Pytela, and D. Sheppard. 1994. Role of the integrin $\alpha_v\beta_6$ in cell attachment to fibronectin. Heterologous expression of intact and secreted forms of the receptor. *J. Biol. Chem.* 269:6940–6948.

Zhou, M.-J., and E.J. Brown. 1993. Leukocyte response integrin and integrin-associated protein act as a signal transduction unit in generation of a phagocyte respiratory burst. *J. Exp. Med.* 178:1165–1174.